Effects of Soil Hygrothermal Properties on the Performance of an Earth-Air Heat Exchanger

Gerson Henrique dos Santos*, Gustavo Chaves Carraro, Victor Vaurek Dimbarre, Thiago Antonini Alves

Federal University of Technology – Parana (UTFPR)
Rua Doutor Washington Subtil Chueire, 330, Ponta Grossa, 84017-220, PR, Brazil;
gsantos@utfpr.edu.br

Abstract. Buildings are responsible for a large part of energy demand worldwide. To collaborate to reduce this demand, the use of passive air conditioning has proven to be beneficial for energy savings. In order to improve thermal comfort in built environments, Earth-Air Heat Exchangers (EAHE) can be installed as a low-cost option. Using low energy consumption, in this system, the ambient air circulates through a pipe buried at a certain depth in the ground, causing it to heat up or cool down, depending on weather conditions. These effects are possible due to the high thermal inertia of the soil. In this context, the climatization performance of EAHE depends directly on the hygrothermal properties of the soil, and the effects of heat, moisture, and air transport on the operation of an EAHE are barely explored in the literature due to many difficulties, such as modeling complexity, computer run time, numerical convergence and highly moisture-dependent properties. Therefore, to analyze the effects of hygrothermal properties of soil, a 2D model has been developed to calculate the coupled heat, air, and moisture transfer. The linearized set of discretized governing equations was obtained using the finite-volume method and solved via the MultiTriDiagonal-Matrix Algorithm, substantially improving the numerical stability and reducing the computer run time. To validate the temperature distribution along EAHE, a prototype was built on the Federal University of Technology of Paraná (UTFPR) - Campus Ponta Grossa, which includes 100 mm diameter Polyvinyl Chloride (PVC) ducts, a fan for airflow control, where a series of k-type thermocouples were inserted along the EAHE. Data were recorded hourly using a data acquisition system during the summer period.

Keywords: Earth-Air Heat Exchanger, Passive Air Conditioning, Hygrothermal Properties of Soils

1 Introduction

The search for sustainable ways to provide air conditioning is currently an important topic in engineering, since nowadays 10% of global greenhouse emissions comes from the cooling services industry, as highlighted by Dong et al [1]. The same authors also mention that as the temperatures worldwide rise and nations get wealthier, the demand for cooling devices is expected to increase. According to the Iternational Energy Agency [2], this demand tends to triple by 2050, with 70 % of the increase coming from the residential sector. Aiming to reduce energy consumption and greenhouse emissions, the Earth-Air Heat Exchanger (EAHE) has emerged as a promising alternative. The EAHE works by allowing air flow through burried pipes in the ground, taking advantage of the thermal inertia of the soil, which maintains a stable temperature along the year at specific depths. As a result, this device can cool the air on hot days and warm it on cold days. According to Greco and Masseli [3], the air outlet temperatures in such devices are not influenced by the burial depth from 1.5 m onwards.

In the literature, several research studies about the subject can be found. Pakari and Ghani [4] investigated an EAHE installed in Doha, Qatar, buried 0.4 m below the surface and extending 21.5 m in length. Their study employed both computational simulations and experimental methods, demonstrating that during summer, the temperature difference between the air inlet and outlet ranged from 5.2 K to 6.8 K. Furthermore, the authors

demonstrated that using this device as a pre-cooler for a conventional air conditioning system could yield annual energy savings of 741 kWh, reducing energy consumption for equivalent cooling power by 64 %. The daily Coefficient of Performance (COP) of the system varied between 6.3 and 17. Khabbaz et al [5] studied an experimental model built at Marrakesh, Morocco, with 72 m in length and burried at 3.2 m depth. The results of the study show that even when the outside air temperature reached 310 K, the outlet temperature of the EAHE was found to be 295 K. Another experimental work, conducted by Zeitoun et al. [6], analyzed the performance of an EAHE built at the University of Strasbourg, France, during the coldest week of 2018 (February 25 to March 3). In this case, the COP of the system was found to range between 2 and 23.5, with the maximum values occurring in the early morning, when the inlet temperatures reach their lowest values, whilst the ground experiences negligible temperature fluctuations.

Regarding numerical studies, Misra et al. [7] set up a 3D model of an EAHE in Ansys Fluent® and evaluated how transient conditions can impair the performance such devices. It was also found that an increase in pipe diameter, inlet air speed and a decrease in the soil thermal conductivity result in a higher loss of performance. Lal [8] employed Ansys Fluent® to develop a 3D model and demonstrated that higher soil thermal conductivity enhances EAHE performance. The author also noted that continuous operation for 12 hours should be followed by a system shutdown lasting 2 to 6 hours, as sustained operation showed decreased performance. Hadi et al. [9] investigated the impact of varying inlet air velocities using a 3D numerical model implemented in Ansys Fluent®. The authors concluded that the system's effectiveness decreases with higher inlet air velocities, as the air requires prolonged contact with the soil for effective heat transfer. The study also emphasized the importance of isolating the air as it approaches the outlet near the surface, where ground temperatures may exceed the air outlet temperature. Sofyan et al [10] analyzed a 3D model set up in Ansys Fluent®, and then verified the effects of the EAHE for cooling purposes in a 36 m² house, being observed that the EAHE was able to reduce the average temperature in the house by 2 K.

As can be seen, the effect of moisture on EAHE performance needs to be explored in the literature. Therefore, to verify the hygrothermal behavior of sandy clay (installation site soil) and backfill soils, a reduced 2D model was developed and implemented in C++ to simulate the coupled heat, air, and moisture transfer in porous soil. The governing equations were discretized using the finite-volume method and then solved using the MultiTriDiagonal-Matrix Algorithm [11], which significantly enhanced numerical stability and minimized computational runtime. The temperature distribution along EAHE was compared to values obtained in a prototype built on the Federal University of Technology of Paraná (UTFPR) - Campus Ponta Grossa.

2 Mathematical Model

The model for the porous soil domain has been elaborated considering the differential governing equations for moisture, air and energy balances. The transient terms of each governing equation have been written in terms of the driving potentials to take more advantage of the MTDMA [11] solution algorithm.

2.1 Moisture Transport

The moisture transport has been divided into liquid and vapor flows as shown in Eq. 1:

$$\mathbf{j} = \mathbf{j}_l + \mathbf{j}_v, \tag{1}$$

where $\mathbf{j}$ is the density of moisture flow rate (kg/m²s), $\mathbf{j}_l$, the density of liquid flow rate (kg/m²s) and, $\mathbf{j}_v$, the density of vapor flow rate (kg/m²s).

The liquid transport calculation is based on the Darcy equation:

$$\mathbf{j}_l = K(\nabla P_{suc} - \rho_l \mathbf{g}), \tag{2}$$

where K is the liquid water permeability (s), P_{suc}, the suction pressure (Pa), ρ_l, the liquid water density (kg/m³) and $\mathbf{g}$ the gravity (m/s²).

The capillary suction pressure can be written as a function of temperature and moisture content in the following form:

$$\nabla P_{suc} = \frac{\partial P_{suc}}{\partial T}\nabla T + \frac{\partial P_{suc}}{\partial P_v}\nabla P_v . \tag{3}$$

Similarly to the liquid flow, the vapor flow is calculated from the Fick's law based equation considering effects of both vapor pressure and air pressure driving potentials:

$$\mathbf{j_v} = \underbrace{-\delta_v \nabla P_v}_{\substack{vapor \\ diffusion}} \underbrace{- \rho_v \frac{k k_{rg}}{\mu_g}\nabla P_g}_{\substack{convective\ \text{vapor} \\ transport}} , \tag{4}$$

where δ_v is the vapor diffusive permeability (s), P_v, the partial water vapor pressure (Pa), ρ_v, the water vapor density (kg/m³), k, the absolute permeability (m²), k_{rg}, the gas relative permeability, μ_g, the dynamic viscosity (Pa.s) and, P_g, the gas pressure.

The water mass conservation equation can be described as:

$$\frac{\partial w}{\partial t} = -\nabla . \mathbf{j}, \tag{5}$$

where w is the moisture content (kg/m³).

This moisture content conservation equation – Eq. 5 – can be written in terms of the three driving potentials as:

$$\frac{\partial w}{\partial \phi}\frac{\partial \phi}{\partial P_v}\frac{\partial P_v}{\partial t} + \frac{\partial w}{\partial \phi}\frac{\partial \phi}{\partial T}\frac{\partial T}{\partial t} = \nabla . \left[-K\frac{\partial P_{suc}}{\partial T}\nabla T - \left(K\frac{\partial P_{suc}}{\partial P_v} - \delta_v \right)\nabla P_v + \rho_v \frac{k k_{rg}}{\mu_g}\nabla P_g + K\rho_l \mathbf{g} \right]. \tag{6}$$

2.2 Air Transport

In the proposed model, the air transport is individually considered through the dry-air mass balance. In this way, the dry-air conservation equation can be expressed as:

$$\frac{\partial \rho_a}{\partial t} = -\nabla . \mathbf{j}_a , \tag{7}$$

with the air flow calculated by the following expression:

$$\mathbf{j}_a = \underbrace{\delta_v \nabla P_v}_{air\ diffusion} \underbrace{- \rho_a \frac{k k_{rg}}{\mu_g}\nabla P_g}_{air\ convection} , \tag{8}$$

where ρ_a is the density of dry air (kg/m³), $\mathbf{j}_a$, the density of dry air flow rate (kg/m²s) and, P_g, the gas pressure (dry air pressure plus vapor pressure) in Pa.

Therefore, the dry air transport can be described as a function of the partial gas and vapor pressure driving potentials so that the air balance can be written as:

$$\frac{\partial \rho_a}{\partial P_g}\frac{\partial P_g}{\partial t} + \frac{\partial \rho_a}{\partial P_v}\frac{\partial P_v}{\partial t} + \frac{\partial \rho_a}{\partial T}\frac{\partial T}{\partial t} = \nabla . \left(-\delta_v \nabla P_v + \rho_a \frac{k k_{rg}}{\mu_g}\nabla P_g \right). \tag{9}$$

2.3 Heat Transport

The heat transfer can be attributed to both conductive and convective effects. The conductive transport is calculated by the Fourier's law:

$$\mathbf{q}_{\mathbf{cond}} = -\lambda \nabla T, \tag{10}$$

while the convective transport can be written as:

$$\mathbf{q}_{\mathbf{conv}} = \underbrace{\mathbf{j}_{\mathbf{l}} c_{pl} T}_{liquid\ flow} + \underbrace{\mathbf{j}_{\mathbf{a}} c_{pa} T}_{dry\ air\ flow} + \underbrace{\mathbf{j}_{\mathbf{v}} L}_{\substack{phase \\ change}} + \underbrace{\mathbf{j}_{\mathbf{v}} c_{pv} T}_{vapor\ flow}, \tag{11}$$

where λ is the thermal conductivity (W/mK), c_{pa}, the specific heat capacity at constant pressure of the dry air (J/kgK), c_{pl}, the specific heat capacity of the water liquid (J/kgK), c_{pv}, the specific heat capacity at constant pressure of the vapor (J/kgK) and, L, the vaporization latent heat (J/kg).

The energy balance equation can be described as:

$$c_m \rho_0 \frac{\partial T}{\partial t} = -\nabla . \mathbf{q}, \tag{12}$$

where c_m is the specific heat capacity of the structure (J/kgK) and ρ_0, the density of the dry material (kg/m³).

In this way, assuming 0 °C as the reference temperature, the energy conservation equation can be written in terms of the three driving potentials as:

$$c_m \rho_0 \frac{\partial T}{\partial t} = \nabla . \begin{pmatrix} \left(\lambda - K \frac{\partial P_{suc}}{\partial T} c_{pl} T\right) \nabla T - \left(K \frac{\partial P_{suc}}{\partial P_v} c_{pl} T + \delta_v c_{pa} T - \delta_v \left(L + c_{pv} T\right)\right) \nabla P_v + \\ \left(\rho_a \frac{kk_{rg}}{\mu_g} c_{pa} T + \rho_v \frac{kk_{rg}}{\mu_g} \left(L + c_{pv} T\right)\right) \nabla P_g + K \rho_l c_{pl} T \mathbf{g} \end{pmatrix}. \tag{13}$$

2.4 Boundary Conditions and Earth-Air Heat Exchanger Model

A 2D reduced model for the soil and heat exchanger domains was tested in the simulations. The soil domain extending 0.5 m in north and south directions from the heat exchanger serpentine was considered. For the dry-air transport, moisture transport, and energy conservation, gas pressure, partial vapor pressure, and temperature have been considered as prescribed values – Dirichlet condition - for the top and bottom surfaces:

$$P_{g,\infty} = P_{g,\text{sup}}, \tag{14}$$

$$P_{v,\infty} = P_{v,\text{sup}}, \tag{15}$$

and

$$T_{\infty} = T_{\text{sup}}, \tag{16}$$

Figure 1 shows the boundary conditions used in the simulations. The thermal resistance of the tube wall was neglected, but it was considered impermeable to moisture flow.

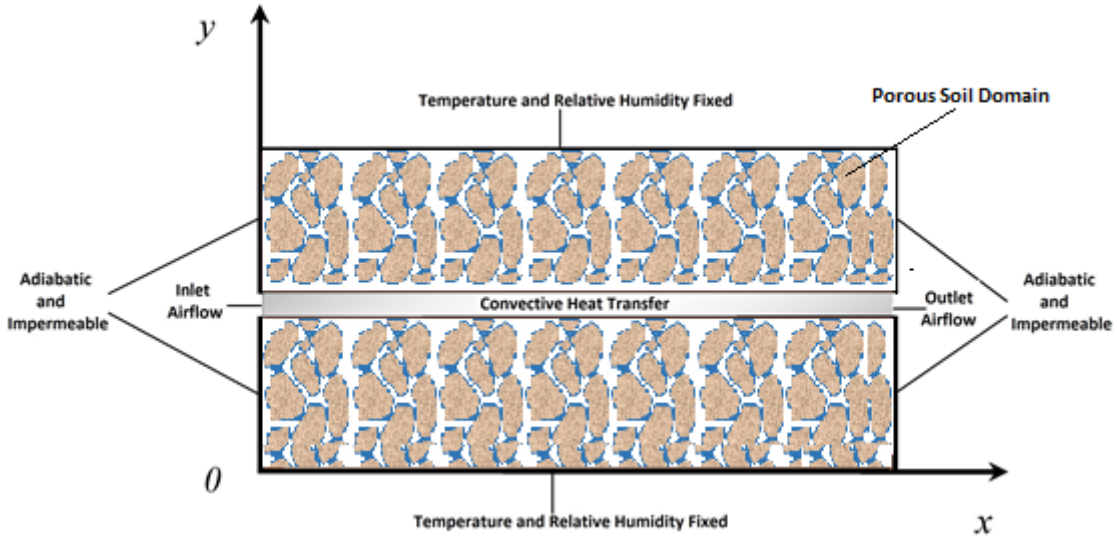

Figure 1. Boundary conditions for the porous soils.

The mathematical model utilized for the Earth-Air Heat Exchanger was proposed by Niu et al. [12]. The main hypotheses adopted were:
- The soil properties are isotropic,
- Air is incompressible and its thermal properties are constant,
- Air is well mixed in the tube with no temperature stratification.

The control volume method was employed in the energy balance for each small volume within the system, as depicted in Fig. 2. In this model, only sensible heat transfer was considered for the air.

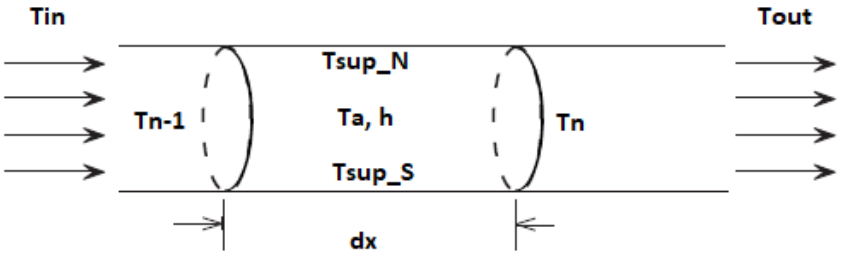

Figure 2. Energy balance in each control volume.

The energy governing equation for each control volume can be written as:

$$\dot{m}\, C\, \mathrm{dT_a} = P\, \mathrm{h}\, (\mathrm{T_S} - T_a)\, \mathrm{dx} \tag{17}$$

where $\dot{m}$ is the mass flow rate of air (kg/s), C, the air specific heat (J/kg K), P, the perimeter (m), and h, the heat transfer coefficient (W/m² K).

The homogeneous ordinary differential equation can be solved analytically as:

$$T_a[i] = T_{avg} - (T_{avg} - T_a[i-1]) \exp(-dx/a), \tag{18}$$

where $T_a[i]$ is the air temperature for each control volume, T_{avg}, the average superficial temperature of tube, and $a = \dfrac{\dot{m}\,\mathrm{C}}{\mathrm{P\,h}}$.

The heat transfer coefficient (h) has been obtained using the Nusselt number (Nu), which was calculated following the Dittus-Boelter equation, valid for turbulent and fully-developed flows through smooth circular pipes:

$$Nu = 0.023 Re^{0.8} Pr^{0.4} \text{(heating)} \tag{19}$$

$$Nu = 0.023 Re^{0.8} Pr^{0.3} \text{(cooling)} \tag{20}$$

3 Simulation Procedure

To obtain the temperature distribution along EAHE, a prototype was built at the Federal University of Technology of Paraná (UTFPR) - Campus Ponta Grossa, which includes 100 mm diameter Polyvinyl Chloride (PVC) ducts, a fan for airflow control, where a series of k-type thermocouples were inserted along the EAHE as verified in Fig. 3.

Figure 3. Prototype built on the Federal University of Technology of Paraná (UTFPR).

Constant temperatures of 24 °C and 23.5 °C and different moisture contents (relative humidity) were imposed on the upper and lower surfaces of the soil domain, which were also obtained experimentally at a depth of 1 m and 2 m. The hygrothermal properties of sandy clay (installation site soil) and backfill were acquired from Oliveira and Freitas [13]. Backfill soil refers to the material used to refill an excavated area once construction or digging activities are completed. It serves several purposes depending on the specific requirements of the project. The basic dry-basis material properties are shown in Tab. 1.

Table 1: Dry-basis properties of soils.

soil	ρ (kg/m³)	*c* (J/kg K)	Porosity (-)
Sandy Clay	1890	1690	0.517
Backfill	2000	850	0.265

4 Results And Discussions

The experimental data analyzed in this work were obtained on January 23 and 24, 2022. The summer of 2021–2022 was mild in Ponta Grossa, Brazil (25.1° South, 50.16° West), and this day corresponded to the highest temperature ranges in the climate for the heat exchanger installation site.

Figures 4 and 5 show the temperature distribution along AEHE for experimental and numerical simulation on January 23 and 24, 2022, at noon. Relative humidity obtained experimentally for clay soil of 50 % (installation site soil) was imposed on the upper and lower surfaces of the soil domain. For analysis of backfill soil performance, relative humidity of 50% and 99.8% were also used in simulations on both surfaces.

Figures 4 and 5 show a maximum difference of 0.8 °C in the outlet of the AEHE, showing a good agreement between the results, even using a simplified model for the soil and heat exchanger. It was also verified that a length of 30 m would be sufficient to maintain the exchanger's performance, considering the climatic conditions of the installation location. When the installation site soil (sandy clay) was changed by backfill and different moisture contents were tested, a slight difference was verified between the values even when a condition close to saturation was used as a boundary condition (RH = 99.8 %). Similar behavior of sorption isotherm curves between the soils could explain these results. The complete and sudden saturation of liquid water only occurs when the relative humidity practically reaches 100%.

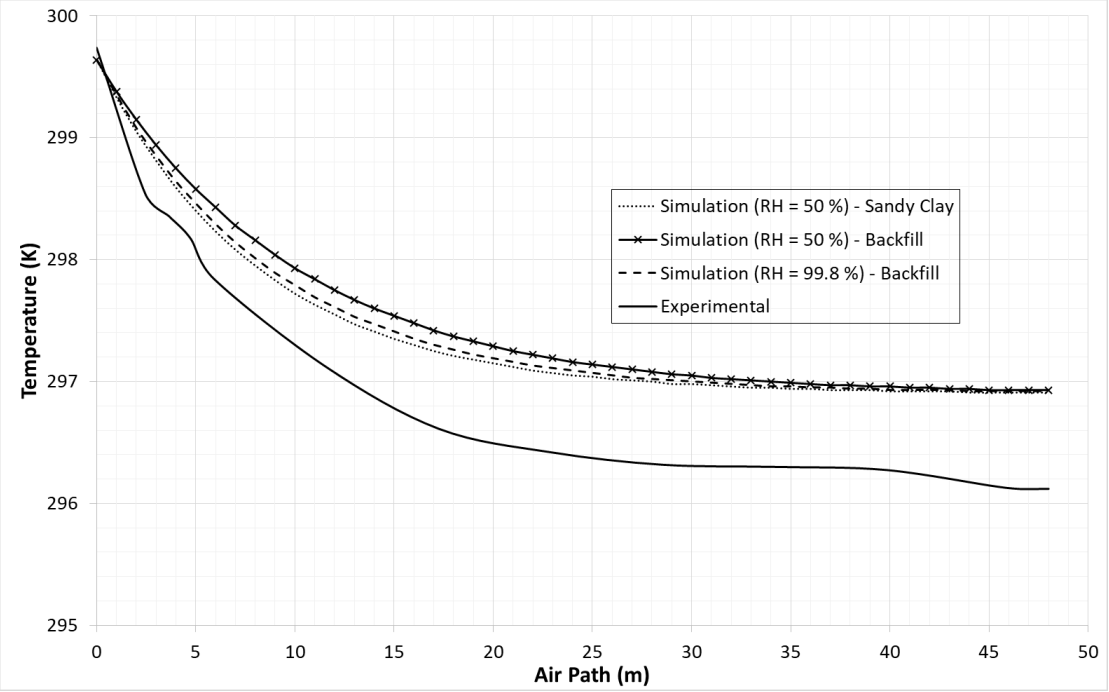

Figure 4. Temperature values on January 23, 2022, at noon.

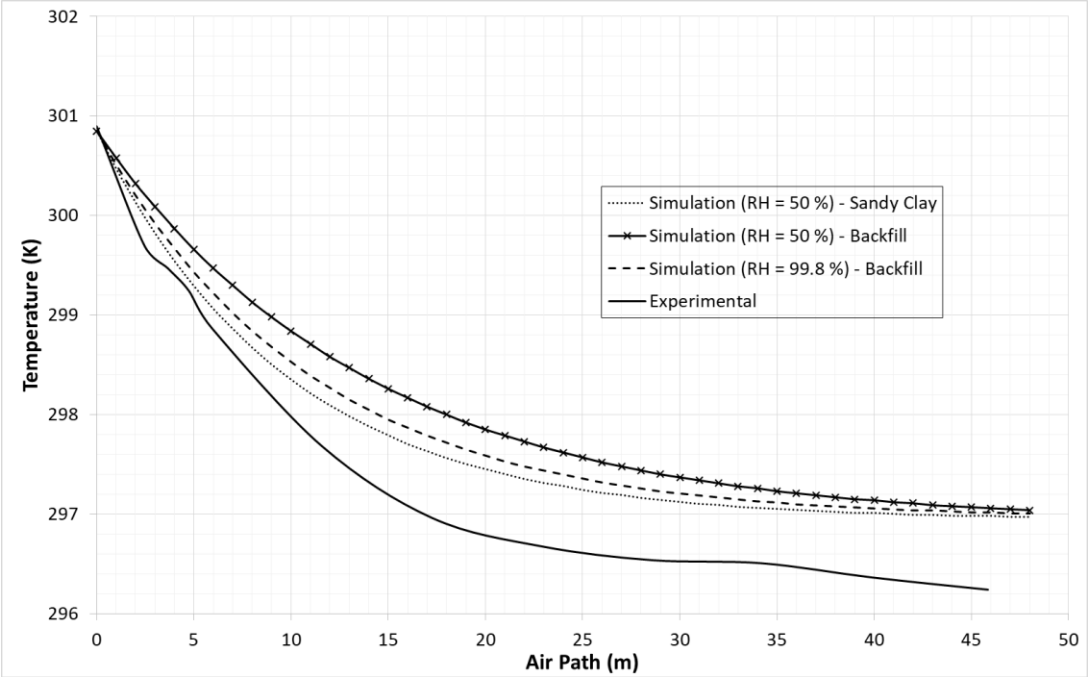

Figure 5. Temperature values on January 24, 2022, at noon.

Figure 6 shows the temperature and vapor pressure profiles for the superior domain of the sandy clay soil on January 24, 2022, at noon. The inferior domain presented symmetric values. The observed gradients of both temperature and vapor pressure indicate that the first 10 meters of the exchanger is the region that could be completely saturated, or different soil configurations for the backfill could be tested in order to increase the heat exchanger's performance.

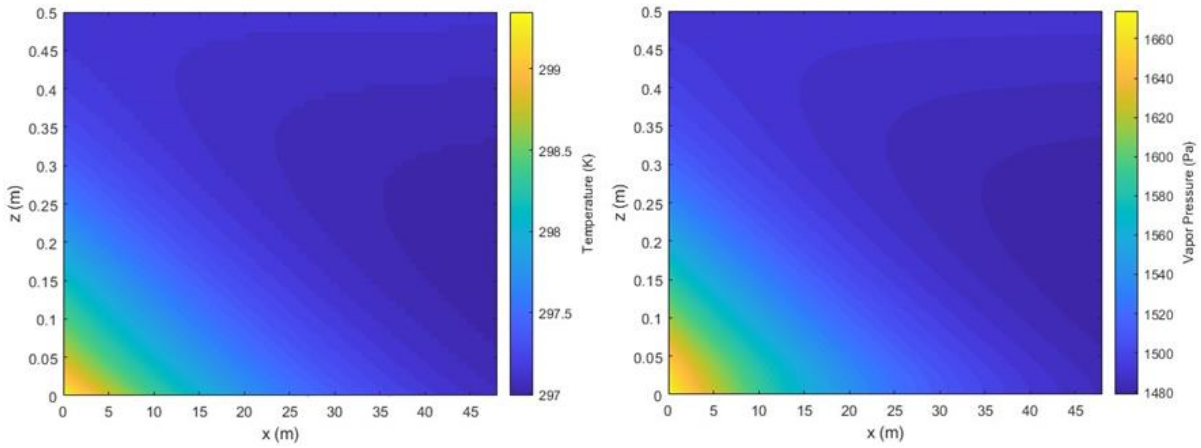

Figure 6. Temperature and vapor pressure values on January 24, 2022, at noon.

5 Conclusions

The effects of the hygrothermal behavior of two different soils in the performance of the EAHE were verified. A 2D reduced model was developed to simulate the coupled heat, air, and moisture transfer in porous soils in order to optimize the computational time consumption. The experimental and simulation values show a good agreement, presenting a maximum difference of 0.8 °C. Sandy clay and backfill soils presented similar hygrothermal behavior due to the same behavior of sorption isotherm curves.

Gradients of both temperature and vapor pressure suggest that the first 10 meters of the exchanger is the region that should explored to increase the heat exchanger's performance. To decrease the space required to install the heat exchanger, the results indicated that a length of 30 meters of serpentine would be sufficient to maintain the air outlet temperature constant for the climatic conditions presented.

In future work, other configurations of the backfill soil will be analyzed with the aim of optimizing the performance of the heat exchanger.

Acknowledgements. The authors thank the National Council for Scientific and Technological Development (CNPq) and the Brazilian Federal Agency for Support and Evaluation (CAPES).

Authorship statement. The authors hereby confirm that they are the sole liable persons responsible for the authorship of this work, and that all material that has been herein included as part of the present paper is either the property (and authorship) of the authors, or has the permission of the owners to be included here.

References

[1] Y. Dong, M. Coleman and S. A. Miller, “Greenhouse Gas Emissions from Air Conditioning and Refrigeration Service Expansion in Developing Countries”. Annual Review of Environment and Resources, pp. 59–83, 2021.
[2] International Energy Agency (IEA). “The future of cooling: opportunities for energy efficient air conditioning”. Paris, 2018.
[3] A. Greco and C. Masselli, “The Optimization of the Thermal Performances of an Earth to Air Heat Exchanger for an Air Conditioning System: A Numerical Study”. Energies, vol. 13, 2020.
[4] A. Pakari and S. Ghani, “Energy Savings Resulting from Using a Near-Surface Earth-to-Air Heat Exchanger for Precooling in Hot Desert Climates”. Energies, vol. 14, 2021.
[5] M. Khabbaz, B. Benhamou, K. Limam, H. Hamdi, P. Hollmuller and A. Bennouna, In: BS2015: 14th Conference of International Building Performance Simulation Association.
[6] W. Zeitoun, J. Lin and M. Siroux, “Energetic and Exergetic Analyses of an Experimental Earth–Air Heat Exchanger in the Northeast of France”. Energies, vol. 16, 2023.
[7] R. Misra, V. Bansal, G. D. Agrawal, J. Mathur and T.K. Aseri, “CFD analysis based parametric study of derating factor for Earth Air Tunnel Heat Exchanger”. Applied Energy, vol. 103, pp. 266-277, 2013.
[8] S. Lal, “Computational Studies of Earth Air Heat Exchanger using CFD: Parametric Analysis”. Journal of Mechanical and Construction Engineering, vol. 3, pp. 1-10, 2023.
[9] F. M. Hadi, M. H. Abed, K. A. Hammoodi, “Thermal Performance of Earth Air Heat Exchanger for Geothermal Energy Application in Hot Climate using CFD Simulation”. Journal of Advanced Research in Fluid Mechanics and Thermal Sciences, pp. 99-117, 2024.
[10] S. E. Sofyan, A. Akram, J. Muhammad, “Development of CFD simulation model of earth air heat exchanger for space cooling of a 36 M2 house in tropical climate Banda Aceh, Indonesia”. Jurnal Polimesin, vol. 21, pp. 170-178, 2023.
[11] N. Mendes, P.C. Philippi, R. Lamberts, “A new mathematical method to solve highly coupled equations of heat and mass transfer in porous media”, International Journal of Heat and Mass Transfer, vol. 45, no. 3, pp. 509–518, 2002.
[12] F. Niu, Y. Yu, D. Yu, H. Li, “Heat and mass transfer performance analysis and cooling capacity prediction of earth to air heat exchanger”. Applied Energy, Vol. 137, pp. 211–221, 2015.
[13] A. A. J. Oliveira, D. S. Freitas, “Influência do Meio nas Difusividades do Modelo de Phillip e Vries”. Research Report, UFSC, 1993.